Solar Energetic Particles and Radio-Silent Fast Coronal Mass Ejections

C. Marqué

Universities Space Research Association, Naval Research Laboratory, 4555 Overlook Av SW, Washington, DC 20375, USA

christophe.marque@nrl.navy.mil

A. Posner

Southwest Research Institute, Space Science and Engineering Division 6220 Culebra Rd., San Antonio, TX 78238 , USA

aposner@swri.org

and

K.-L. Klein

LESIA, Observatoire de Paris, 5 place Jules Janssen, 92195 Meudon Cedex, France

ludwig.klein@obspm.fr

ABSTRACT

Both solar flares and shock waves driven by fast coronal mass ejections (CMEs) can accelerate charged particles in the solar corona and create transient enhancements of solar energetic particle (SEP) fluxes in interplanetary space, known as SEP events. Since fast CMEs and flares often occur together, it is difficult to directly identify the actual source of the SEPs detected near Earth orbit. In this paper, we attempt to single out fast CMEs without any signature of particle acceleration related to a flare. In order to minimize effects of occultation by the solar limb, we choose meter wave radio emission from energetic electrons as a tracer of flare-related particle acceleration, because this emission arises at greater coronal heights than X-rays or centimetric radio waves. In truly radio-silent fast CMEs, where the absence of metric radio emission is not due to limb occultation, the only source of SEP acceleration should be the shock wave driven by the CME.

In a systematic search in the early CME catalog of the SoHO/LASCO coronagraph (St. Cyr et al. 2000) for fast CMEs (V$>$ 900 km.s^{-1}) located above the western solar limb between July 1996 and June 1998 we found 24 fast CMEs, of which only three were radio-silent. Comparison of their speeds with the fast magnetosonic speed in the corona shows that these three CMEs very likely drive coronal shock waves, and that their properties do not depart significantly from a reference set of SEP-associated fast CMEs, except for their angular width, which is smaller. Although one, possibly two of the three radio silent CMEs are accompanied by weak enhancements of the electron and proton fluxes ($E_p < 20$ MeV) observed by the particle detectors COSTEP aboard SoHO and EPAM aboard ACE, none produces a conspicuous SEP event. This suggests that either efficient particle acceleration at CME shocks occurs over much smaller angular ranges than generally believed or that the shock is not as efficient a particle accelerator at energies above $\sim$10 MeV as often thought.

Subject headings: Sun: coronal mass ejections (CMEs), flares, particle emission

1. Introduction

The Sun generates transient fluxes of non thermal particles (SEP: Solar Energetic Particles) in interplanetary space, ranging from suprathermal to relativistic energies. Different contexts of particle acceleration have been identified. Fast coronal mass ejections (CMEs) drive shock waves which can accelerate electrons and ions within a large volume of the corona and interplanetary space. Flares, i.e. small-scale processes of energy conversion within active regions, are known to provide efficient particle acceleration as inferred from gamma-ray, hard X-ray and microwave observations (see the reviews by Aschwanden (2002); Vilmer & MacKinnon (2003)). Statistical relationships have been observed between SEP intensities and CME speeds in the plane of the sky (Kahler et al. 1984, 1987; Simnett et al. 2002; Gopalswamy et al. 2004) as well as between intensities of escaping electrons and, with more scatter, protons and the soft X-ray peak flux of the associated flare (Gopalswamy et al. 2004). The latter association suggests a relationship between the escaping SEPs and small-scale energy release in the flaring active region well behind the CME shock. The identification of the particle accelerator in SEP events is thus not possible on the sole ground of statistical association. Other distinctive criteria such as charge states and elemental abundances are also not fully conclusive (Labrador et al. 2003). The recent discovery that fast, but narrow CMEs may be associated with impulsive SEP events (Kahler et al. 2001), and that in these events protons up to several tens of MeV that promptly escape to 1 AU are accelerated

behind the CME front and its presumed shock (Klein & Posner 2005) further complicates a picture which once (Reames 1999) was believed to provide a clear distinction between flare-accelerated small impulsive SEP events and CME shock-accelerated large gradual ones.

A probe of shock-accelerated SEP events would be cases where the contribution of other acceleration sites but the CME shock is excluded. Kahler et al. (1986) discussed a flareless particle event associated with the eruption of a quiescent prominence to show that the fast CME (speed about 840 km.s^{-1}) associated with the prominence eruption was able to accelerate ions up to several tens of MeV/nuc, and electrons up to MeV energies. To our knowledge this remains the only event where flares seemed to be absent, although even this was questioned more recently (Cane et al. 2002). In the present study, an attempt is undertaken to single out, among all fast CMEs thought to generate a coronal and interplanetary shock wave, those which are NOT accompanied by signatures of particle acceleration by other processes in the corona, but the CME shock. The aim is to see if these CMEs produce SEP events, and if so, in which energy range. Metric radio bursts, radiated by non thermal electrons at heights between roughly 0.1 and 1 $R_\odot$ above the photosphere, are used as an indicator of flare-related particle acceleration in the corona. This radiation is preferable to X-rays for two reasons: it is clearly non thermal, and, because of the height of emission, it is less easily occulted by the limb. We call "radio silent" those CMEs which are not accompanied by metric radio bursts, and where the absence of such bursts is not due to occultation by the limb.

The outline of the paper is as follows: in Section 2 a list of all fast CMEs observed between July 1996 and June 1998 above the western solar limb by the *Large Angle Spectroscopic Coronagraph* (LASCO, Brueckner et al. 1995) on the *Solar and Heliospheric Observatory* (SoHO) mission, is compiled from the LASCO CME catalog. Among 24 CMEs, only three radio-silent ones have been identified after elimination of events where the absence of radio emission is likely the result of occultation (Sect. 2.1). The CMEs and the coronal activity during these three events are presented in Sect. 2.2, together with the proton signatures at 5-55 MeV detected by the *Comprehensive Suprathermal and Energetic Particle Analyser* (COSTEP; Müller-Mellin et al. 1995) aboard SoHO. It is shown that either a weak or no particle signature is found. In the discussion, we give an estimate of the magnetosonic speed in the corona and of the strength of the CME shocks, using models of the coronal density and magnetic field. We then compare the speeds and Mach numbers, as well as the pre-event conditions and other CME parameters of radio-silent and SEP-related CMEs.

2. Observations

This study relies on the identification of rapid coronal mass ejections (CMEs) from observations with the LASCO coronagraphs aboard the ESA/NASA SoHO mission. From St. Cyr's list of CMEs observed by LASCO (St. Cyr et al. 2000), available via the LASCO homepage[1], those observed above the western solar limb with projected speed above $900\,\mathrm{km.s^{-1}}$ were selected. In order to avoid confusion in periods of high activity, we restricted our systematic research of events to the period from July 1996 to June 1998.

Activity in the solar corona was monitored at extreme ultraviolet wavelengths (Fe XII line, 19.5 nm) by the *Extreme Ultraviolet Imaging Telescope* (EIT) aboard SoHO (Delaboudinière et al. 1995), at soft X-rays by the *Soft X-ray Telescope* (SXT) aboard the YOHKOH spacecraft (ISAS, Tsuneta et al. 1991), and the whole Sun monitor aboard the *Geostationary Orbiting Environmental Satellites* (GOES, NOAA). The data were provided through the web pages of the CME catalog, the EIT instrument[2], and the Solar Data Analysis Center (SDAC)[3], all at Goddard Space Flight Center. Radio observations of the corona were carried out with the Nançay Radioheliograph (henceforth NRH; Kerdraon & Delouis 1997). Observatory reports in *Solar Geophysical Data* (NOAA; henceforth SGD) were used to identify Hα flares and the spectral type of metric radio emission.

[1]http://lasco-www.nrl.navy.mil/

[2]http://sohowww.nascom.nasa.gov/

[3]http://umbra.nascom.nasa.gov/

Table 1a. Fast west-limb CMEs July 1996 - June 1998 accompanied by flares, and associated particle signatures (ACE/EPAM protons and electrons, IMP 8 protons). The first column is the temporal rank of the 24 events (first event is presented in Tab. 1b). The second column gives the date and, within parentheses, the day of the year. The reference time of a CME refers to the first image of LASCO/C2 where it is visible. The sixth column gives a brief indication on the specific flare signature of the event.

Event #	CME Event Date,time (DOY)	Speed [km s^{-1}]	ACE/ EPAM	IMP8	Comment
2	1997 Oct 07, 13:30 UT (280)	1300	E4, P1-8 50, dg	50, dg	no Hα, no EUVb, no X, AR far behind SW limb; radio: pure II (Klein et al. 2003)
3	1997 Nov 06, 12:10 UT (310)	1600	E4, P1-8	>500, 4.3	Hα S18 W63, X9.4, radio III, II, IV, (Maia et al. 1999; Reiner et al. 2000)
5	1998 Mar 29, 03:48 UT (088)	1500	no event	not rep.	no Hα, no EUVb, radio IV
6	1998 Mar 31, 06:12 UT (090)	2100	E4, P1-8	···	Hα S21 E50, C1.4, radio III, DCIM
7	1998 Apr 06, 05:04 UT (096)	910	ongoing	not rep.	no flare, no X (but: SXT loops behind SW limb ?), radio III, II
8	1998 Apr 20, 10:07 UT (110)	1600	E4, P1-8	>120, 8	no Hα, no EUVb (dimming >W limb), M1.8, radio II, IV, flare behind limb (Klassen et al. 2002; Bastian et al. 2001)
9	1998 Apr 29, 16:58 UT (119)	1000	E4, P1-8	70, 0.009	Hα S17 E22, M6.8, radio III, II, IV
10	1998 May 02, 14:06 UT (122)	1000	E4, P?-8	500, 1.1	Hα S15 W16, X1.1, radio DCIM, IV, (Warmuth et al. 2000; Pohjolainen et al. 2001)
11	1998 May 06, 08:04 UT (126)	1100	E4, P?-8	500, 1.4	Hα S15 W64, X2.7, radio III, II, IV
12	1998 May 08, 06:27 UT (128)	1400	ongoing	not rep.	Hα N23 W57, M1.6, radio III, II, IV
13	1998 May 09, 03:35 UT (129)	1700	E4, P1-8	>120, 0.08	no Hα, EUVb $\geq$W limb, M7.7, radio III, II, IV
14	1998 May 09, 20:04 UT (129)	1300	ongoing	not rep.	no Hα, no EUVb (dimming >W limb), C4.0, radio III
17	1998 May 12, 08:55 UT (132)	1100	ongoing	not rep.	Hα S24 W02, no X, radio III
19	1998 May 27, 13:37 UT (147)	960	E4, P?-8	50, 0.001	Hα S23 W83, C7.5, radio IV (Klein et al. 2005)
22	1998 Jun 16, 18:27 UT (167)	1600	E4, P1-8	70, 0.01	no EUVb, M1.0 (>SW limb, SXT), radio III, II
23	1998 Jun 20, 07:57 UT (171)	940	ongoing	not rep.	Hα N33 W50, SXTb, SXT loops >NW limb, radio: noise storm onset

2.1. Event selection

This study considers only CMEs observed above the western limb or halo CMEs whose speeds are measured above the western limb, in order to guarantee optimum propagation conditions to the Earth for particles accelerated during these events. 24 events have speeds above 900 km.s^{-1}. They are listed in Table 1.a (CMEs associated with flare signatures) and 1b (CMEs without accompanying flare signature). The second column gives the date (day of the year in parentheses) and the time when the CME is first detected in the field of view of the LASCO-C2 coronagraph, i.e. at heliocentric distances above 2.2 $R_{\odot}$. The third column gives the CME speed in the plane of the sky from St. Cyr's catalog, rounded off to two significant figures. When a very different - in all cases significantly smaller - speed is reported in the CME catalog covering the complete SoHO mission lifetime (Yashiro et al. 2004) [4], St. Cyr's value is quoted within parentheses.

The fourth column gives the energy channels where the *Electron, Proton and Alpha Monitor*(EPAM) aboard the *Advanced Composition Explorer* (ACE) mission (Gold et al. 1998) detects the associated particle event[5]. The particle event is associated with the CME when the electrons and the fastest protons observed appear to rise near the first time the CME is seen in the C2 images. In these cases the energy channels where the event is detected are indicated. E4 designates the electron channel in the (175-312) keV energy range, while the proton channels range from P1 (47–65 keV) to P8 (1.91-4.75 MeV). The qualification "ongoing" means that a previous event exists, and no new particle injection related with the CME under discussion can be identified. "No event" means that the particle channels show no excess above background.

The fifth column lists the maximum proton energy (MeV) at which the event is detected by IMP 8, and the maximum intensity measured in the range (24-29) MeV, in units of (cm^2 s sr MeV)$^{-1}$. The values are drawn from the list of SEP events compiled by Cane et al. (2002). The term "not rep." means that no event is reported with the specific CME by these authors, while "dg" refers to data gap.

The "Comment" column gives the type of flare-related activity around the time when the CME is first observed. This comprises metric radio emissions and Hα flares reported in SGD or, when no Hα event is reported, brightenings in SoHO/EIT and YOHKOH/SXT daily movies, designated "EUVb" and "SXTb", respectively, in the Table. Metric emission is characterized by the burst type: Type III bursts are produced by electron beams propagating

[4]http://cdaw.gsfc.nasa.gov/CME_list

[5]http://www.srl.caltech.edu/ACE/ASC/level2/index.html

Table 1b. Fast west-limb CMEs July 1996 - June 1998 with no or questionable indication of an associated flare. The projected speed of the CME (from St. Cyr's catalog) is put within parentheses when a significantly lower value is indicated in Yashiro's catalog. In the sixth column, "RS" means radio silent, "O" means that no disk signature of the CME was detected in SoHO/EIT images so that the CME most likely occurred well behind the west limb.

Event #	CME Event Date,time (DOY)	Speed [km s^{-1}]	ACE/ EPAM	IMP8	Class	Comment
1	1996 Nov 28, 16:50 UT (333)	970	... [a]	not rep.	O	no Hα, no EUVb (but: EIT loops behind W limb): C1.3, no radio patrol
4	1998 Jan 03, 09:42 UT (003)	980	E4, P1-8	not rep.	RS1	filament eruption; no Hα, no EUVb, no radio
15	1998 May 10, 14:07 UT (130)	(990)	ongoing	not rep.	F?, O	no Hα, no EUVb, C1.0, radio III (?)
16	1998 May 11, 14:27 UT (131)	(920)	ongoing	not rep.	O	no Hα, no EUVb, no X, no radio
18	1998 May 13, 05:27 UT (133)	1200	no event	not rep.	O	no Hα, no X, no radio
20	1998 Jun 02, 08:08 UT (153)	(1400)	E4, P1-8	not rep.	RS2	fil. erupt., no Hα, no EUVb (but: EIT loops behind SW limb), (Plunkett et al. 2000), no radio
21	1998 Jun 04, 02:04 UT (155)	1700	E4, P1-8	40, 0.0002	O	no Hα, no EUVb, radio CONT (?)
24	1998 Jun 20, 18:20 UT (171)	1000	ongoing	not rep.	RS3	no Hα, no X, no radio

[a]before ACE launch

upward into the high corona and interplanetary space. Type IV emission is a broadband continuum lasting more than 10 minutes, up to several hours, which reveals time-extended electron acceleration in the corona. Type II bursts are the characteristic radio signature of electrons accelerated at a shock wave. Radio phenomena are described in detail in McLean & Labrum (1985). See Pick (1986) and Mann et al. (1995) for discussions of type IV and type II emission, respectively.

Half of the fast CMEs (12/24) are accompanied by flares as revealed by Hα, EUV or soft X-ray emission; all of them have radio signatures at meter wavelengths, too. In four others the only flare signatures are metric radio waves, including one event occurring behind the limb (1997 October 7, (Klein et al. 2003)). The greater number of events with metric radio signatures of flares meets our expectation that such radio emission is less easily occulted than other flare signatures. The absence of metric radio emission in the eight CMEs of Table 1b is due either to occultation of activity far behind the western limb or to the absence of electron acceleration in the corona. We anticipate the distinction between occulted events (labelled "O" in the fifth column of Table 1b) and truly radio-silent CMEs (labelled "RS") from Sect. 2.2. Inspection of the Tables shows that all major particle events that occur with fast CMEs are also associated with flares (Table 1a), although not all fast CMEs with flares actually produce SEP events. Only one of the fast CMEs without signatures of coronal particle acceleration (Table 1b) is accompanied by a particle event detected by IMP-8. It is the weakest of the IMP 8 events associated with the CMEs of our sample.

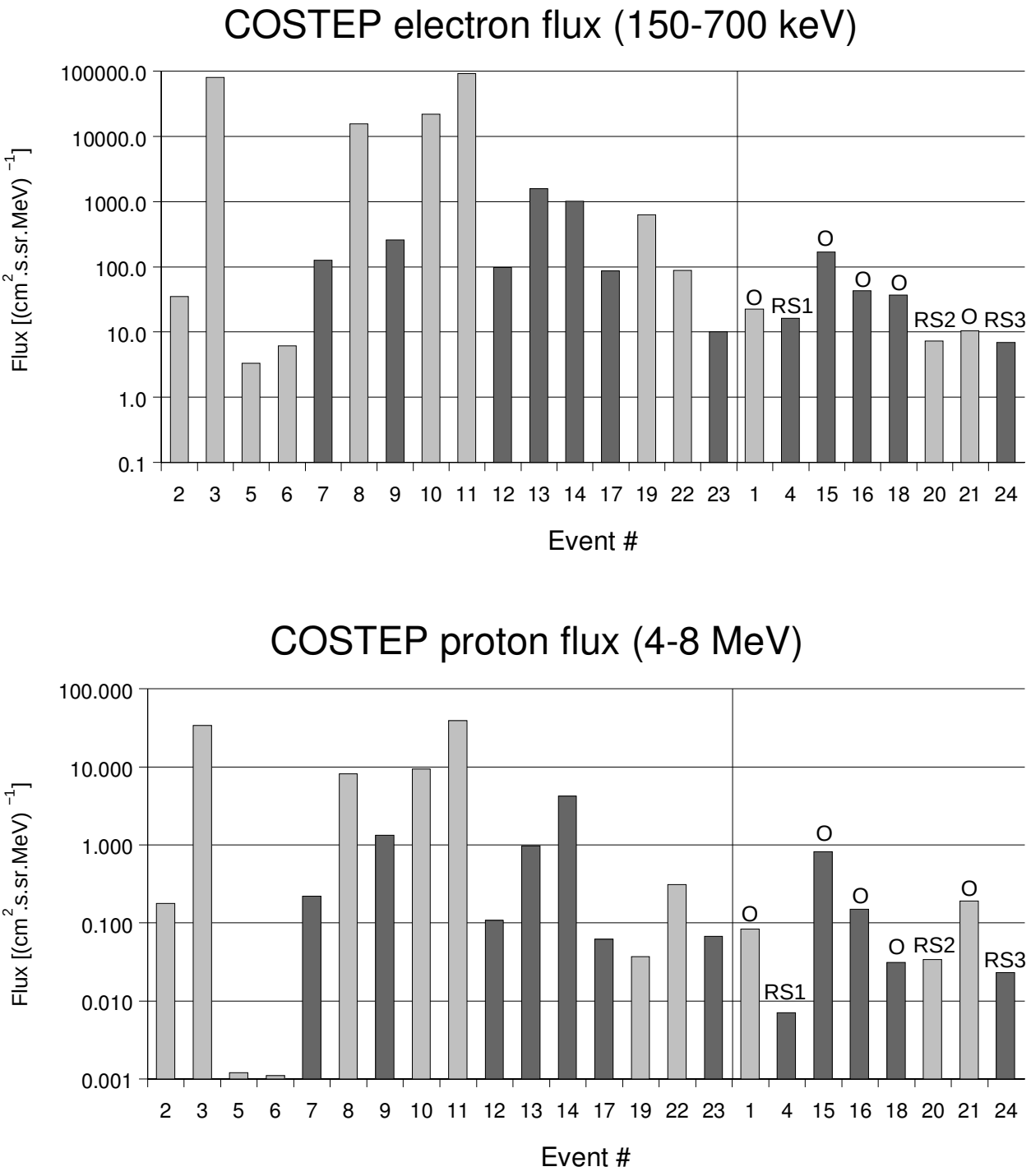

Fig. 1.— SoHO/COSTEP measurements for the CME events of Tables 1a and 1b; the event numbers are identical to the ones used in these two Tables. A dark gray bar indicates that the event occurs while a high background level of particles is detected. Occulted and radio silent events are labelled respectively 'O' and 'RS'.

Fig. 1 presents the electron and proton maximum flux measurements from the SoHO/COSTEP instrument for the sample of CMEs of Tables 1a and 1b. The two populations are displayed on the same plot, separated by a vertical line, and each event is referenced by its number in Tables 1a and 1b. For clarity, occulted ('O') and radio silent CMEs ('RS') are indicated; the distinction being explained in the next section. The dark gray bars identify those CMEs which occur during a high background from a previous particle event. In these cases the height of the bar mainly reflects the background level. About half of the CMEs occur while the background level of particles is high, including occulted or radio silent CMEs. In the following, we investigate in more details these three radio silent CME events.

2.2. Radio silent CMEs

For the eight CMEs of Table 1b, without metric radio emission, the coronagraphic images taken by LASCO (C2) are compared with EIT images in the search of activity other than flare-related brightenings. When no changes are detected in the EIT images during some tens of minutes before the appearance of the CME in the LASCO C2 field of view, we considered that the CME occurred far behind the solar limb, such that even metric radio emission revealing particle acceleration in the corona, behind the CME, may be occulted. This inspection leads to the identification of three CMEs, two are associated with filament eruptions near or at the limb, as seen with EIT, and one with some activity near the west limb, observed with YOHKOH/SXT. These three CMEs, which we refer to as "radio silent" in the following (identified as RS1, RS2 and RS3 in Fig. 1 and Table 1b), can therefore be safely considered as being not entirely confined to the backside of the Sun. If they drive a shock wave, particles are expected to be accelerated on magnetic field lines connected with the Earth.

The trajectory of the leading edge of these CMEs was measured in the LASCO images. We derived from a linear fit the time when the CME front was at the limb, and the average speed. These speeds and those at heliocentric distances of 2 and 20 $R_\odot$ as derived from parabolic fits are listed in Table 2, together with the central position angle of the CME (PA) and its width. Linear speeds from the catalogs of St. Cyr and Yashiro are given in cols. 9 and 10. The minimum western longitude where EIT or YOHKOH sees activity is given in col. 11. The solar wind speed measured by Wind/SWE (1998 January 03 and June 02) or ACE/SWEPAM (1998 June 02 and 20) is used to compute the connection longitude of the nominal interplanetary Parker spiral, listed in the last column of Table 2.

Comparison with the linear speeds from the catalogs of St. Cyr and Yashiro (cols. 9, 10 of Table 2) shows a wide range of speeds measured by different authors for a given CME.

This discrepancy most likely arises from the different methods used to estimate the CME velocity. Our own measurements are made using full resolution LASCO images, and trying to track and follow a given structure from one image to the other. Yashiro's catalog (Yashiro et al. 2004) on the other hand is based on half-resolution images and running difference movies that highlight the biggest extent of the CME, but do not allow to follow the same structure from one image to the other. In that sense, it gives a different description of the event which is not necessarily close to the information published in St Cyr's catalog (St. Cyr et al. 2000). We have on purpose omitted any error bars in these measurements, due to this large discrepancy, because we believe that all the speed measurements relative to these CMEs are valid and describe accurately the velocity range of individual structures.

Although our own measurements give the lowest speeds, we would like to point out that the mean speed of all CMEs of 1998 is 421 km.s^{-1} according to Yashiro et al. (2004), and that a limit of 400 km.s^{-1} is a common criterion used to distinguish fast and slow CMEs (see for example Cliver et al. (1999) or Sheeley et al. (1984)). In other words, these radio silent CMEs are fast events.

Table 2. Properties of the radio silent coronal mass ejections: extrapolated times when the front is at 1 $R_\odot$ heliocentric distance (linear fit), central position angle and width, speed estimates, and the minimum longitude where coronal perturbations are visible in EIT or YOHKOH (June 20) images.

Event	Date (1998)	Time (UT) at 1 $R_\odot$	PA	Width	Speed [km.s^{-1}] linear	2 $R_\odot$	20 $R_\odot$	St. Cyr	Yashiro	Minimum longitude	Connection longitude
1	2	3	4	5	6	7	8	9	10	11	12
RS1	Jan 03	09:11	290°	85°	670	634	764	978	1020	40°	62°
RS2	Jun 02	09:29	245°	59°	725	-	1260	1383	751	48°	57°
RS3	Jun 20	07:27	292°	53°	805	778	857	943	909	50°	55°

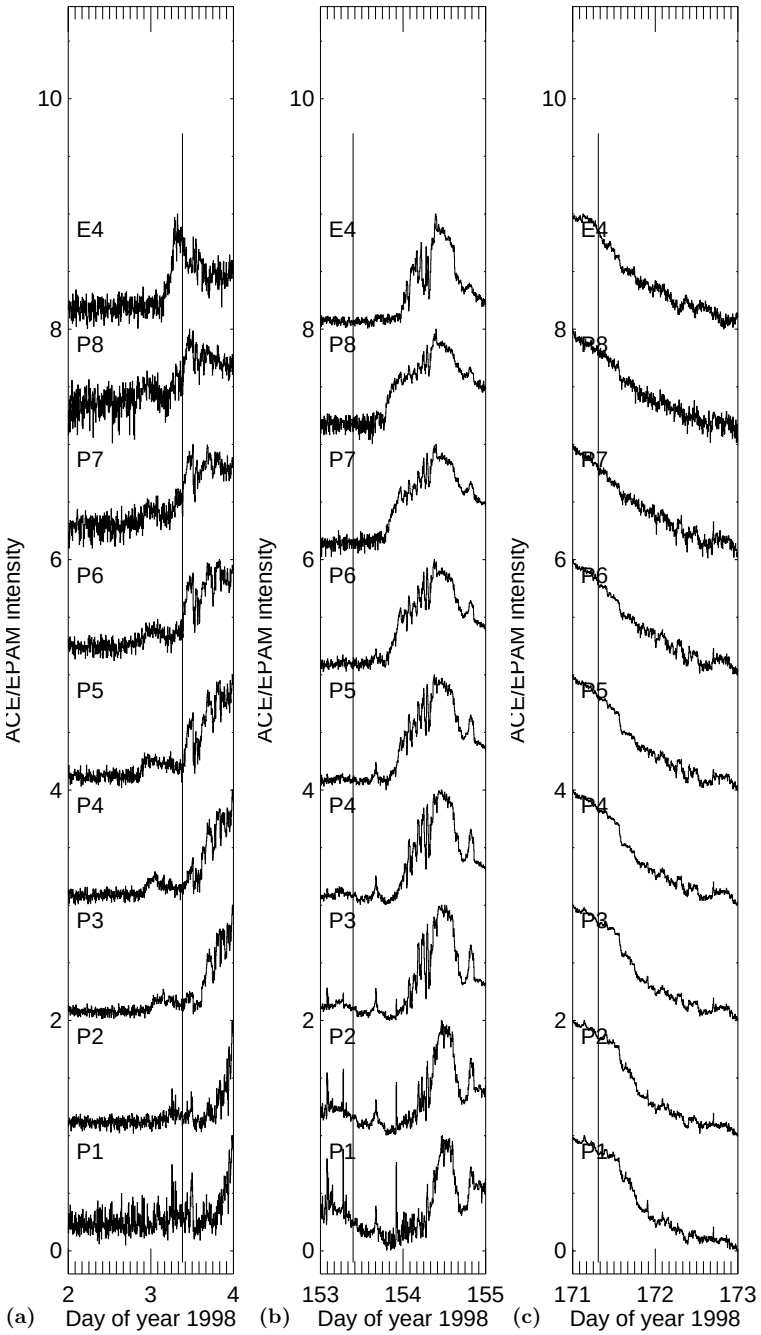

Fig. 2.— Time histories of particle fluxes (logarithmic scale) detected during three radio silent CMEs by ACE/EPAM: (a) RS1: 1998 Jan 03, (b) RS2: 1998 Jun 02, (c) RS3: 1998 Jun 20. The uppermost curves (labelled E4) show electrons in the energy range (175–312) keV. Below are the proton channels in eight contiguous energy ranges from (1.91-4.75) MeV (P8; second curve from top) down to (47-65) keV (P1; bottom curve). The vertical lines indicate the times when the backward extrapolated positions of the CME fronts pass at the projected heliocentric distance of 1 $R_\odot$ (see Table 2).

Two of the three radio silent CMEs (RS1 and RS2), are accompanied by particle events seen by ACE/EPAM. The count rate time histories of mildly relativistic electrons ((175–312) keV, curves at the top) and of protons in eight energy channels between 47 keV and 4.75 MeV are plotted in Fig. 2. The particle event in Fig. 2a shows a clear velocity dispersion of the onset times, which points to a start before the radio silent CME (see below). Later on, the time profile may suggest a contribution from the radio silent CME RS1, but this point remains open. The onset of the second event (Fig. 2b) is obscured by a magnetic cloud, while EPAM sees the decrease of a previous event at the time of third one (Fig. 2c), with no unambiguous trace of a fresh injection that is correlated with the onset and early phase of the CME RS3. None of these events is detected by the GOES instruments. In the following section we present the three events in more detail, including measurements as to which energies the spectra of the three solar energetic particle events detected by ACE actually extend.

2.3. Individual events

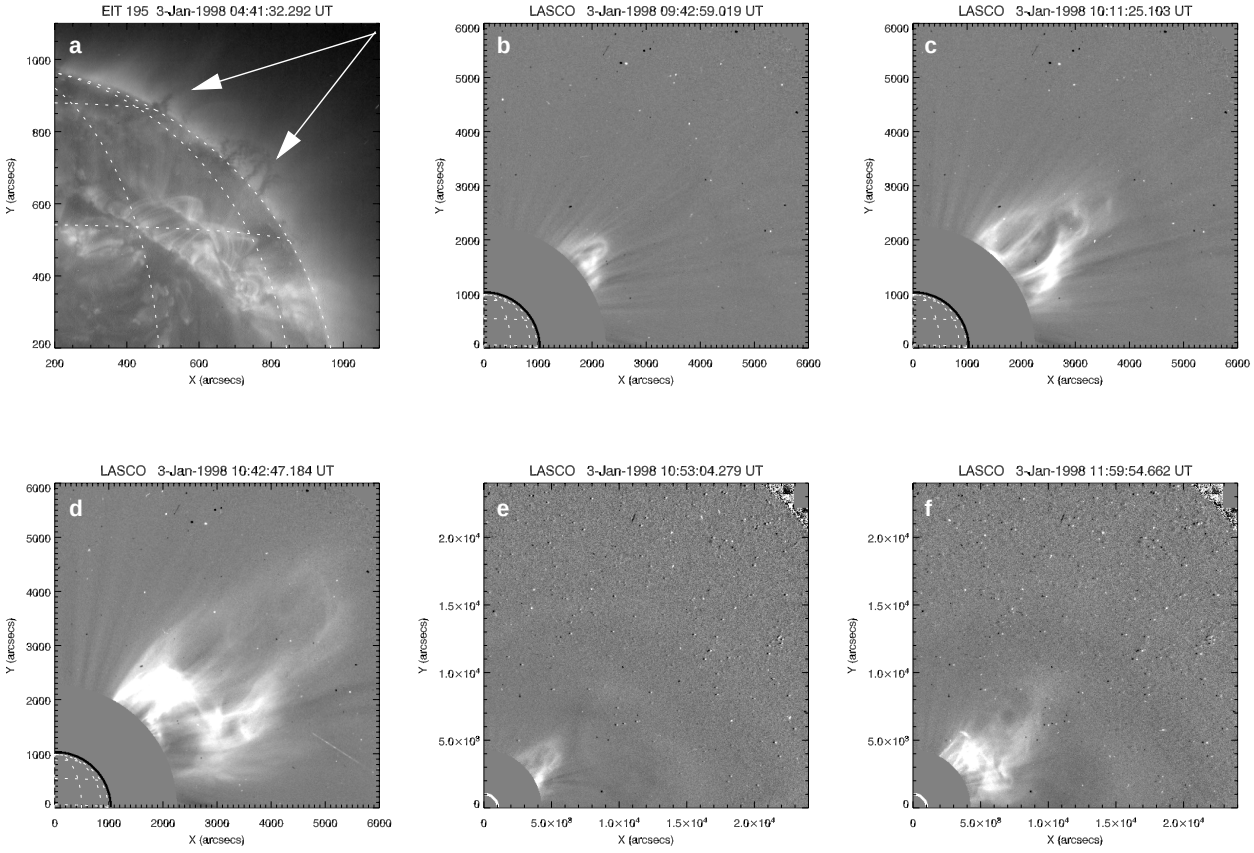

Fig. 3.— SoHO/LASCO images taken during the coronal mass ejection RS1 on 1998 January 03 and of low coronal activity by SoHO/EIT. (**a**) EIT image at 19.5 nm (Fe XII). The two arrows point to prominences which erupt during the event. (**b-d**) LASCO C2 images. (**e-f**) LASCO C3 images. A pre-event image has been subtracted from the LASCO images. In the C3 images the brightest stars have also been subtracted.

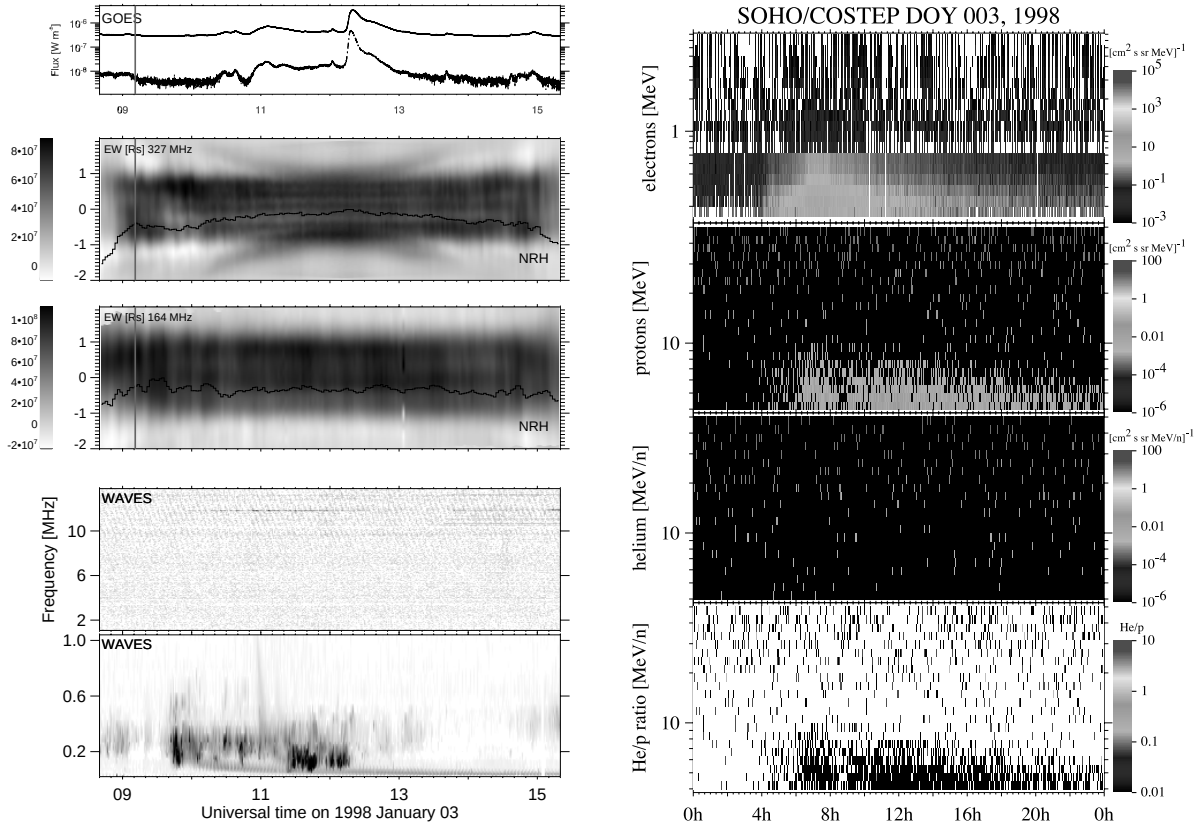

Fig. 4.— Time histories of soft X-ray, radio emission and particle detection during the rise of the 1998 January 03 CME. Left, from top to bottom: (i) whole Sun flux in the two energy channels (0.12-0.8) nm and (0.05-0.4) nm of GOES 10, (ii) one-dimensional projection of the radio brightness at 327 and 164 MHz onto the solar east-west direction (reverse color table: dark shading shows bright emission; ordinate graded in solar radii from Sun center, with negative values referring to the Eastern hemisphere), (iii)dynamic spectra of the whole Sun radio emission between 14 MHz and 1.075 MHz. The vertical line at 09:11 UT shows the time when the extrapolated trajectory of the CME front passes 1 $R_\odot$ from disk center. The apparent rise and decay of the meter wave radio emission near 08:30 UT and 15 UT is an instrumental artefact, and the apparent oscillations of the source are due to gravity waves in the terrestrial ionosphere. The broad radio emission in this Figure is thermal emission of the quiet corona. Right: spectrograms of energetic particles detected on SoHO by COSTEP (see the online edition for a colour version of this figure); from top to bottom: 150 keV - 8 MeV electrons, 4 - 50 MeV/n protons and helium, and the ratio of helium to protons.

2.3.1. RS1 event: 1998 January 03

The CME and its associated low coronal activity are displayed in Fig. 3. In the EIT image (Fig. 3.a) a system of post flare loops is seen in the foreground. These loops develop beginning at 0:00 UT and are not related to the event under consideration. The two arrows point to filaments on the limb. The southwestern one shows structural changes during several hours before erupting. It is no longer seen in the EIT image taken at 09:20 UT. The north-eastern filament erupts near 10:30 and becomes a bright prominence during the eruption. While it erupts, an arcade of loops starts to develop on the disk, and then extends southward across the north-western limb over $\sim 40°$, between approximately 40°and 80°of longitude (west). This gives a rough idea of the length of the eruptive filament system.

The activity related with the CME clearly has a counterpart on the disk. The CME observed by LASCO (Fig. 3.b-f) has a complex shape with much fine structure in its front. This complicates the identification of a single feature that can be tracked through LASCO's field of view, and probably accounts for the wide dispersion of the speed measurements in Table 2.

The time history of soft X-ray and metric-to-kilometric radio emissions is plotted on the left hand side of Fig. 4. A series of minor fluctuations after 10 UT and the flare of soft X-ray class C3.3 at 12:12 UT may be associated with the prominence eruption and post flare loop formation at the north-western limb. No Hα flare is reported in *SGD* (Comprehensive Reports) at this time. At the time of this flare, i.e. 3 hours after the instant when its backward extrapolated location is at the limb, the CME front is 10 $R_\odot$ from Sun center. While the EIT and GOES observations show signatures of post-eruptive reconnection in the aftermath of the CME, at meter waves (327 and 164 MHz, for illustration) only quiet Sun emission is seen from the time when the CME front is at 1 $R_\odot$ until the end of the NRH observations, when the front is 22 $R_\odot$ from Sun center. The one-dimensional brightness time histories in Fig. 4 (second and third panel from top) are grey-scale plots with reverse color scale (black shading means bright emission). They represent the brightness, integrated over the solar north-south direction, as a function of the solar east-west position (West on top). The ordinate is graded in units of the solar radius, 0 marks the center of the disk. The figures show a nearly uniform band of emission between the eastern and the western limb. This is the thermal emission of the quiet corona. Fluctuations of the position of the broad source are generated in the Earth's ionosphere. The cross-shaped feature on top of the quiet Sun at 327 MHz is an instrumental artefact.

No radio signature at any wavelength from ~ 1 cm to several meters is reported by whole Sun patrol instruments between 01:30 and 17:00 UT on this day in *Solar Geophys. Data*. It appears that the triggering and rise of the CME through the corona is not accompanied by

electron acceleration up to at least 1 $R_\odot$ above the photosphere. The dynamic spectra taken by *WAVES/Wind* below 14 MHz (two bottom panels of Fig. 4) reveal a faint type III burst near 11:00 UT, which is visible below 1 MHz, but there is no conspicuous emission at higher frequencies. The ongoing bursts at frequencies below 0.6 MHz are not of solar origin.

Displayed on the right hand side of Fig. 4, COSTEP sees a dispersionless rise of proton count rates at energies up to 7 MeV near 04:00 UT, but no new release during the time when the CME traveled through the corona. A minor Hα flare is reported in *SGD* at 04:35 UT, N22 W55, but no metric radio emission. The enhanced proton flux at COSTEP lasts several hours, with a short interruption near 9 UT. It cannot be excluded that the radio silent CME contributes to the particle flux after this interruption, but there is no indication from the velocity dispersion in the COSTEP or the EPAM (Fig. 2.a) data that this is actually the case. Whatever the contribution of the radio silent CME to the proton signatures at ACE and SoHO, it does not extend to energies above 7 MeV.

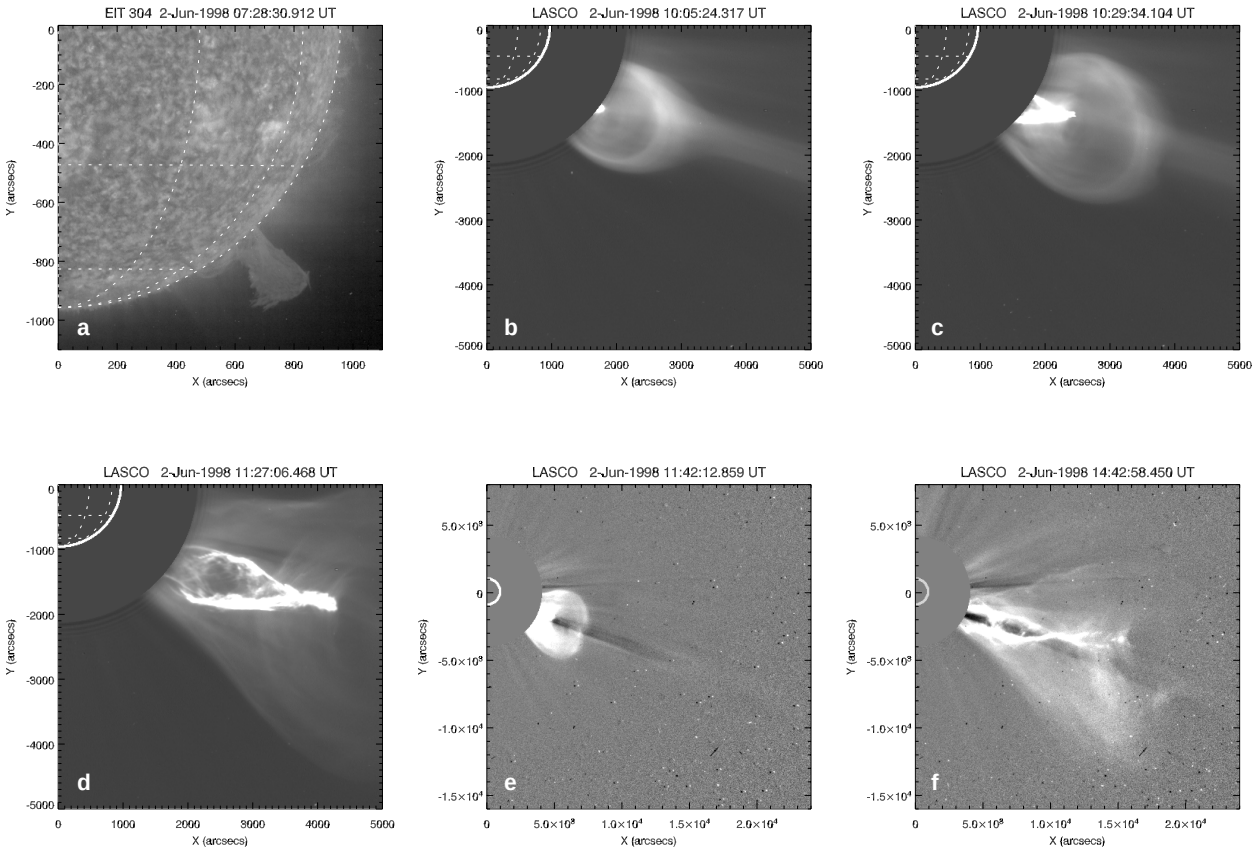

Fig. 5.— SoHO/LASCO images taken during the coronal mass ejection RS2 on 1998 June 02 and of activity in the lower corona by SoHO/EIT. See Fig. 3. The EIT image is at 30.4 nm (He II). No pre-event image has been subtracted for the LASCO-C2 data.

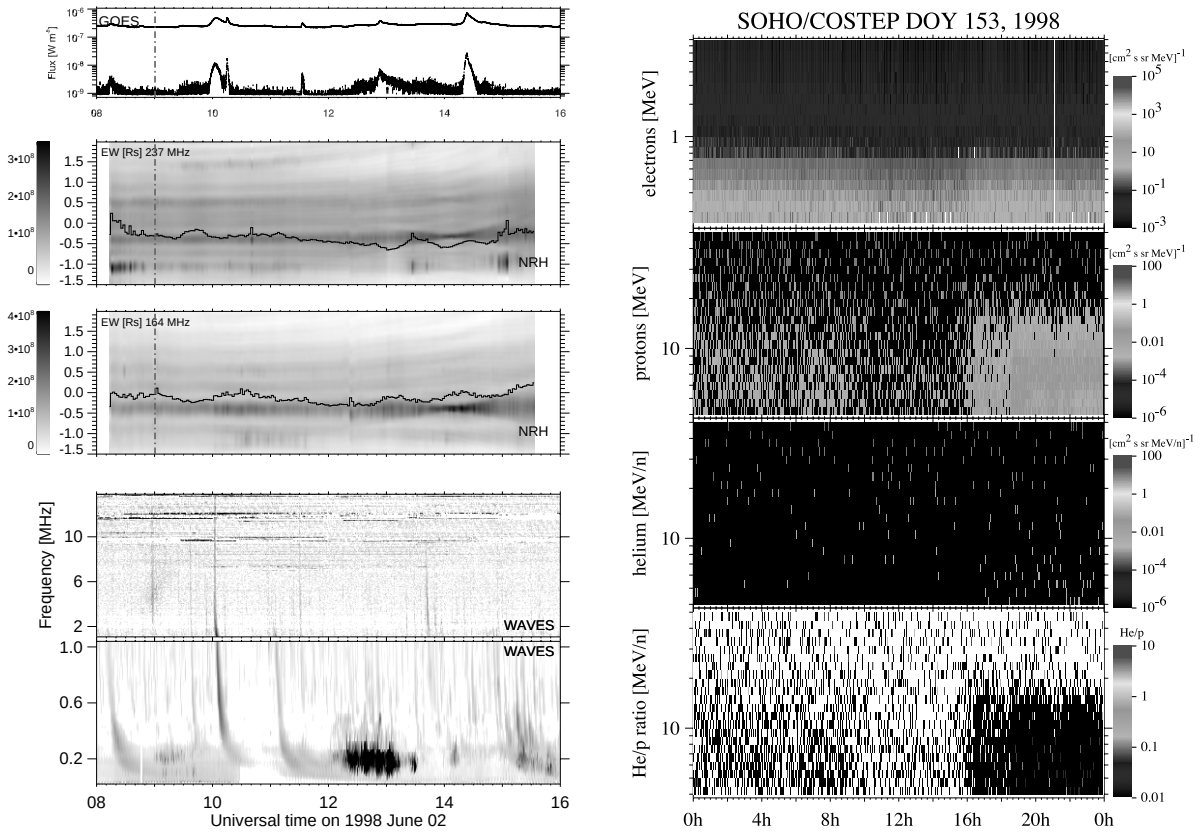

Fig. 6.— Time histories of soft X-ray, radio emission and particle detection during the rise of the 1998 June 02 CME. See Fig. 4.

2.3.2. RS2 event: 1998 June 02

The CME and the embedded untwisting prominence (Fig. 5) have been extensively discussed in Srivastava et al. (1999) and Plunkett et al. (2000). The event is associated with the eruption of a quiescent prominence near the south western limb.

Its rise starts between 6:00 UT and 7:00 UT in the EIT 19.5 nm images. Figure 5.a shows the prominence at 30.4 nm during its eruption. Starting near 11:00 UT, arcade loops develop above the limb, but some brightenings occur also within the limb down to $\sim 50^\circ$ of longitude West. The arcades continue rising and spreading until about 18:00 UT and then fade. Snapshots of the CME with the embedded prominence as a bright feature are displayed in the LASCO images of Figs. 5.b,c, while Fig. 5.d illustrates the helical structure of the prominence at a later time.

While the CME travels through the corona, several faint soft X-ray bursts are observed by GOES (Fig. 6). The tiny event shortly after 08:00 UT is associated with an Hα subflare at S27 E43 (Kanzelhöhe Observatory, SGD 652-II). The one at 10:00 UT is accompanied by a decametric-to-hectometric type III burst (henceforth DH type III burst), but no Hα flare is reported, and no distinct brightening is visible in the EIT 19.5 nm daily movie. The main meter wave emission seen by the NRH (Fig. 6) is a noise storm in the eastern hemisphere, revealing the time-extended acceleration of electrons to suprathermal energies (a few keV). The DH type III burst near 10:00 UT occurs together with a temporary enhancement of this noise storm. This activity is unrelated with the CME above the south-western solar limb. At no time during the interval when the CME front is between the solar limb and 15:30 UT, when it is 23 $R_\odot$ away from the disk center, does a radio signature of non thermal electrons show up in the observations of the western solar hemisphere by the NRH (Fig. 6) or in patrol observations reported in *Solar Geophys. Data*.

At COSTEP, a simultaneous (non-dispersive) rise of particle count rates is observed near 16 UT up to an energy of at most 20 MeV. Magnetic field measurements at WIND[6] (Ogilvie et al. 1995) show that the spacecraft is within a magnetic cloud between 10:30 and 15:54 UT (cf. also Vilmer et al. 2003). It is therefore likely that the enhanced proton fluxes are those of a solar energetic particle event associated with the CME, the onset of which is not visible because SoHO is in the same magnetic cloud. When SoHO exits the cloud, the low-energy electron channel of COSTEP sees a minor increase of electrons up to 400 keV. Note that minor electron event decay times are small and a higher ($\times 10$) flux is likely at event onset. Also, COSTEP observes excess flux of protons ($0.034\,(\mathrm{cm^2\,s\,sr\,MeV})^{-1}$) at 4-8

[6]http://lepmfi.gsfc.nasa.gov/mfi/windmfi.html

MeV. This flux might have been only slightly higher ($\times 2$) at event onset due to the usually larger proton event decay times.

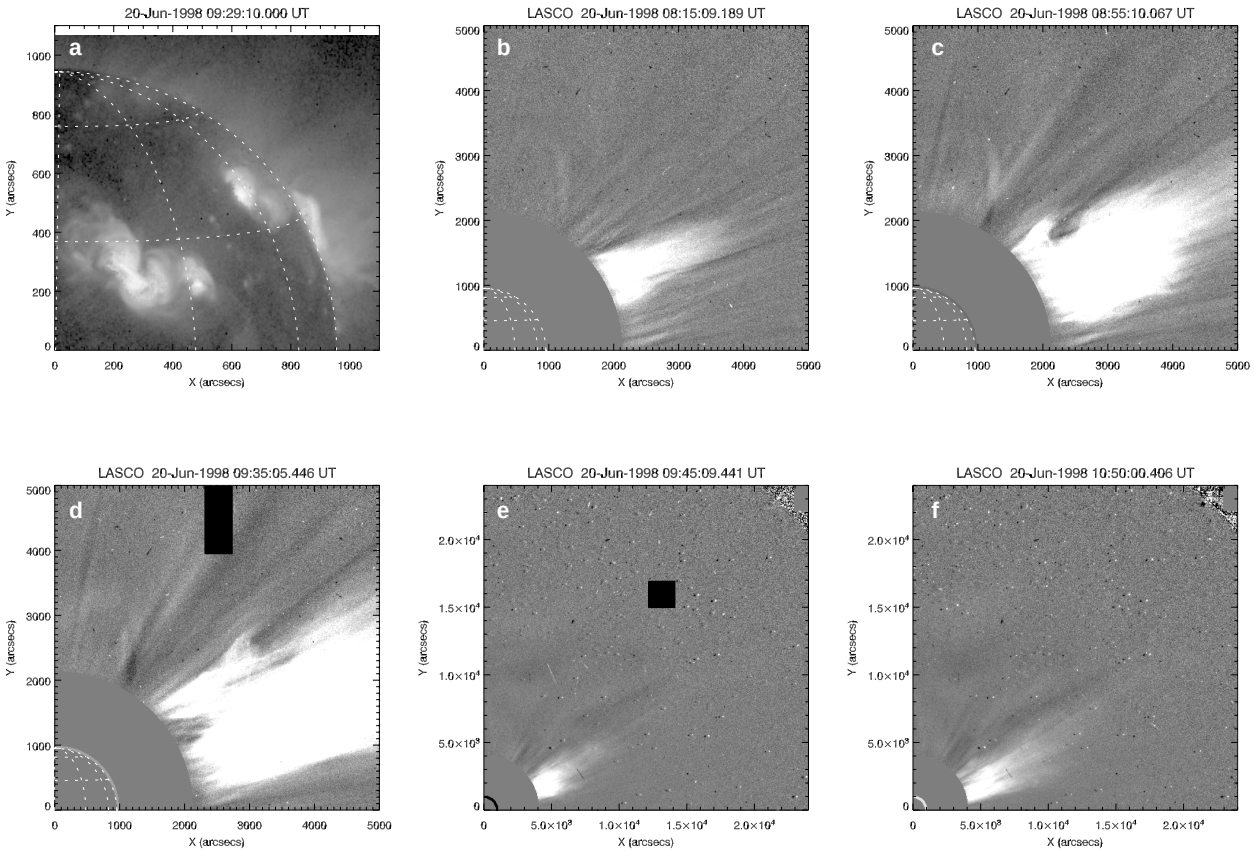

Fig. 7.— SoHO/LASCO images during the coronal mass ejection RS3 on 1998 June 20 and of activity in the lower corona by YOHKOH/SXT (**a**). Note that the SXT image has been taken after the start of the CME. See Fig. 3.

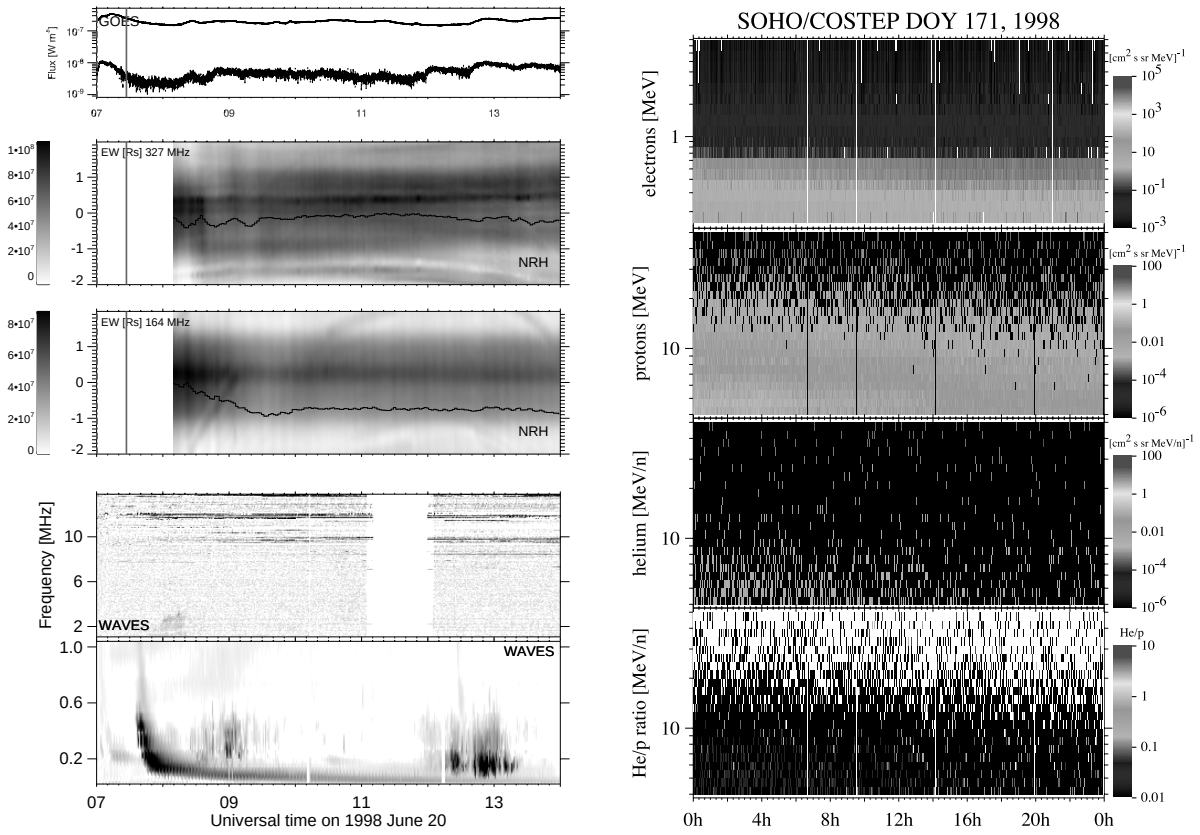

Fig. 8.— Time histories of soft X-ray, radio emission and particle detection during the rise of the 1998 June 20 CME. See Fig. 4

2.3.3. RS3 event: 1998 June 20

Fig. 7 and 8 summarize the solar and particle activity related to this radio silent CME. An Hα subflare is observed at Kanzelhöhe at 07:11 UT (N33 W50, SGD 652-II), but the whole Sun soft X-ray fluxes show no event from the onset of the CME to 14 UT when its front is 28 $R_\odot$ from Sun center (Fig. 8). However, YOHKOH/SXT sees (post-) flare loops from a site behind the north-western limb since 07:21 UT, starting together with compact brightenings at similar latitudes, south-west and north-east of active region NOAA 8244 (N35 W54, SGD 648 I). The soft X-ray loops rooted behind the limb brighten at 07:38 and again near 09 UT (see Fig. 7.a), and subsequently evolve over several hours (SXT movie provided by Yashiro's CME catalog). There are no NRH observations at the time when the CME starts to rise. Later on metric emission (Fig. 8) is essentially that of the quiet corona, with a faint noise storm slightly west of the central meridian. No signature of electron acceleration is seen related to the evolving flare loops at the north-western limb seen by YOHKOH/SXT.

A weak hectometric-to-kilometric type III burst occurs at frequencies below about 1 MHz near the onset of the CME, possibly associated with the flare at 07:11 UT, but no evidence for coronal electron acceleration is seen afterward. A 1N flare with soft X-ray and broadband radio signatures is reported at 14:19 UT from N14 W23 (SGD).

COSTEP sees a slightly enhanced background from a previous event, but no new release during this day.

3. Discussion

In this study we have investigated the SEP signature of radio-silent fast CMEs, i.e. fast CMEs which are not accompanied by metric radio emission. Only CMEs which occurred close to the western limb as shown by simultaneous EUV or X-ray imaging of coronal structures were considered, so that it is unlikely that either the radio emission went undetected because it was occulted, or the particle events went undetected due to unfavorable magnetic connectivity. We therefore consider that radio silence at metric wavelengths means there is no electron acceleration due to magnetic restructuring behind the CME in the corona. We assume in the following that the absence of electron acceleration also implies that no ions are accelerated, i.e. that there is no energetic particle source during these events that competes with acceleration at the bow shock expected to be driven by these CMEs. Only three such CMEs were identified above the western limb between July 1996 and June 1998. Radio silent fast CMEs are clearly rare events. None of the three radio-silent fast CMEs was associated with SEP enhancements measured by the GOES spacecraft. Particle signatures

were detected aboard SoHO (COSTEP) and ACE (EPAM) in association to one, possibly two, of these CMEs. The situation is unclear in the latter case because a different event started a few hours earlier. No enhanced particle fluxes were seen with the third radio silent CME.

We identify four possible interpretations for the absence or weakness of SEP signatures during these events:

- Radio-silent CMEs are too slow to drive sufficiently strong shock waves. We discuss this interpretation in Sect. 3.1, where we conclude it is not consistent with the observations.
- Shocks are driven by these CMEs, but encounter unfavorable conditions for particle acceleration in the corona (seed population). This is discussed in Sect. 3.2, where no significant difference is found in this respect between radio-silent CMEs and CMEs associated with conspicuous SEP events.
- Shock waves are produced in these CMEs, but are too narrow to intercept the interplanetary magnetic field line connected with the spacecraft. This is discussed in Sect. 3.3
- Shock waves are driven by radio-silent CMEs and intercept the Earth-connected field line, but accelerate SEP only up to a few tens of MeV at best, and to low intensities.

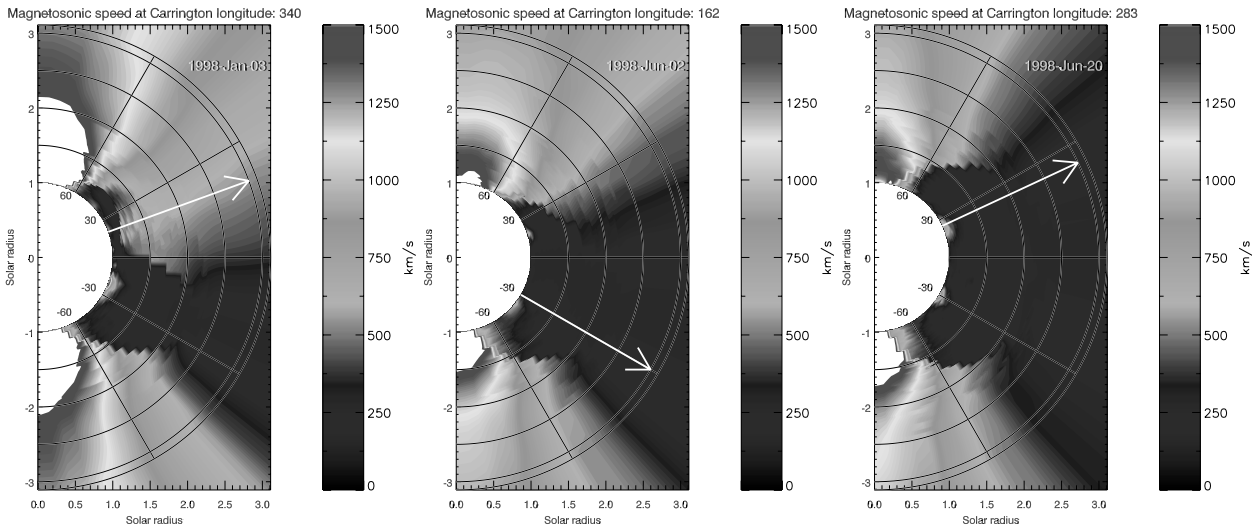

Fig. 9.— Distribution of the the fast magnetosonic speed for the three radio silent CMEs. The white arrow points out the mean direction of the CME. (See the online edition for a colour version of this figure)

3.1. Magnetosonic speeds and Mach numbers

Fast CMEs can trigger shock waves in the corona. In Section 2.2, we have shown that our sample of radio-silent CMEs were faster than average, but ultimately, local physical conditions determine the shock efficiency of a CME. In the following, we evaluate the magnetosonic fast mode speed in the background corona through which the CMEs propagate.

Estimations of the Alfven speed profile in the corona are usually based on simple analytical magnetic field models (Mann et al. 2003; Gopalswamy et al. 2001). Although useful to discuss under which conditions a shock may be produced, they do not reflect the local coronal conditions that vary from one event to the other. In order to describe more accurately the fast magnetosonic speed distribution in the corona, we use here a method developed by Wang (2000) to study the propagation of EIT waves in the low corona. The coronal magnetic field is extrapolated from a synoptic map of photospheric measurements, assuming a potential field in the corona with a source surface at distance 2.5 $R_\odot$ from the center of the Sun (Wang & Sheeley 1992). In this model, the base density N_0 varies according to the strength of the photospheric field B and the loop length L: $N_0 \propto B.L^{-0.5}$, and obeys a hydrostatic profile with constant electron temperature $T = 1.5 \times 10^6$K (Wang 2000). The altitude range of the model is 1-3.11 $R_\odot$ from the center of the Sun.

The fast magnetosonic speed distribution has been computed for each of the three radio-silent events. Figure 9 displays the result of the model in the plane of the sky, above the west limb, where the CMEs have been identified. The outer circle marks the upper boundary of the model, and any value above that limit is an extrapolation. A white arrow points out the direction of the CME propagation in the plane of the sky.

In order to investigate the ability of these CMEs to drive a shock, we have computed the fast magnetosonic Mach number profile, along the trajectory of the CME, using the CME speed measurements from this study, as well as Yashiro's and St Cyr's catalogs. The results are summarized in Table 3.

Table 3. Minimum, maximum and final values at 3 $R_\odot$ of the fast magnetosonic Mach number for the radio silent CMEs on the limb; the corresponding heliocentric distance of the minimum and maximum of the Mach number are also provided.

Event	Date	This paper	St Cyr	Yashiro	Heliocentric distance	Value at 3 $R_\odot$ This study, St Cyr, Yashiro
RS1	1998 Jan 03	0.9-3.3	1.3-4.7	1.3-5.0	1.16-1.14	1.2-1.8-1.9
RS2	1998 Jun 02	2.4-3.9	4.6-7.4	2.5-4.0	1.0-2.3	3.6-6.8-3.7
RS3	1998 Jun 20	1.1-4.2	1.3-5.0	1.2-4.8	1.0-2.1	3.6-4.3-4.1

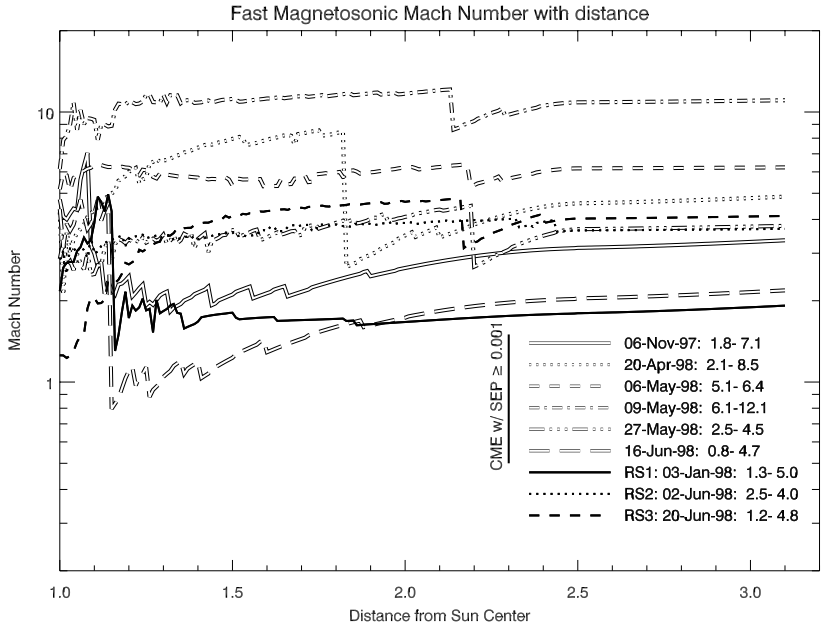

Fig. 10.— Magnetosonic Mach numbers as a function of heliocentric distance r up to $r = 3R_\odot$, for radio silent CMEs and for SEP associated CMEs. The Mach number is obtained by dividing the CME speed inferred from a linear fit by the fast magnetosonic speed in the corona, assuming propagation along a radial along the central position angle of the CME. The CME velocities were found in Yashiro's catalog.

The Mach number estimates deduced from our velocity measurements or the ones tabulated in the CME catalogs (see Table 3) reveal that the three radio silent CMEs are likely to be shock associated within the altitude range 1-3.1 $R_\odot$. Therefore the lack of conspicuous SEP event may not be explained by the absence of a coronal shock, but it is possible that the strength of this shock is too low compared to the ones associated with CMEs for which SEPs are observed. To test this hypothesis, we have computed the fast magnetosonic Mach numbers of the CMEs listed in Table 1a for which a proton flux ≥ 0.001p.$(cm^2.s.ster.MeV)^{-1}$ was detected on IMP8. Two CMEs, event #9 and #10 have been discarded because the longitude where these events originate from is too close to the central meridian to give a reliable CME velocity measurement.

To make this comparison, we used Yashiro's speed measurements (Yashiro et al. 2004) for both groups of events. Fig. 10 presents the profile of the Mach number with distance, along the mean direction of the CME propagation, above the associated active region if applicable (in that case we have corrected the linear speed for the longitude-projection effect), or on the limb (for the three radio silent CMEs, thick curves). For each event, we have indicated the minimum and maximum value of the Mach number in the insert. The large steps observed in the profiles mark the boundary between closed and opened field area. No clear difference shows up between the three radio silent CMEs and the SEP-associated CMEs, in terms of Mach number in the low corona (below 3 $R_\odot$). With the exception of the 1998 May 9 event, which displays an extremely high Mach number due to the unusual speed of the CME (v$\sim$ 2330 km.s^{-1}), the radio silent and SEP associated CMEs have very similar fast magnetosonic Mach numbers, all above a value of one within 3 $R_\odot$.

From this comparison, it appears that the strength of the shocks associated with the selected CMEs is established and remains rather constant at heliocentric distances above $\sim 2\,R_\odot$. Therefore, the strength of the shock at low altitude does not seem to be a decisive factor in the SEP productivity of a CME.

The true 3D geometry of the CMEs is of course unknown and one cannot exclude that the properties of the shock are longitude-dependent. For example, if we apply our "conservative" measurements of the radio-silent CME speed on the limb to compute the Mach number profile at smaller longitudes, one of the event (January 3rd 1998) can propagate at sub-Alfvenic speeds along most of its trajectory, due to the electron density profile at these longitudes, whereas the two other CMEs remain super-Alfvenic. This emphasizes the need of a 3D velocity field for a given CME, which could be provided by the future STEREO mission.

3.2. The pre-event corona in radio silent and SEP-associated CMEs

Recent research has emphasized that the pre-event corona could be of crucial importance to the question if, at which intensity, and with which composition SEP events are observed at the Earth. E.g., Kahler (2001) concludes that SEP intensities are higher in the presence of enhanced background intensities (measured immediately before the onset of the SEP event; note, however, that the correlation is very weak in the scatter plots in his Fig. 3). Two of the three radio silent CMEs occur during an enhanced flux of energetic particles from a previous event. The previous event is clearly seen at COSTEP energies on 1998 Jan 03 (RS1 CME), and is sufficiently strong as to mask the possible contribution of the radio silent CME. There is no previous SEP event on June 02 (RS2 CME), but ACE/EPAM (Fig. 2) and COSTEP show the decline of a previous event on June 20 (RS3 CME). Hence suprathermal seed particles are available at the time when the presumed CME shock travels through the corona on 1998 Jan 03 and Jun 20. There is no evidence for such a population from the EPAM observations on June 02. Minor flares occur near the western limb between May 28 and May 29, but no conspicuous activity is reported in *SGD* from the vicinity of the erupting prominence. There is thus no evidence for suprathermal seed particles in this event, but the situation is not fundamentally different from the solar activity in the western hemisphere prior to the fast CME of 1998 April 20, which is associated with a conspicuous SEP event.

Another potential influence of the ambient corona is suggested by Gopalswamy et al. (2004) who show that SEP intensities are enhanced when the trajectory of the associated CME intersects that of a previous one. The trajectories of the three radio silent CMEs in our sample also cross those of previous CMEs. Furthermore, Richardson et al. (2003) show that the time of the presumed interaction of CMEs in general lags behind the SEP event onset. So whatever the nature of the CME interaction suggested by the intersection of the trajectories, it is not a necessary condition for an SEP event to occur.

In summary, the radio silent CMEs of Table 2 are neither particularly isolated nor do they occur on an unusually quiet background.

3.3. The widths of radio-silent and SEP-associated fast CMEs

The only apparent difference between the radio-silent CMEs and those associated with SEP events in Tables 1a is the width. The widths of the five CMEs in this Table that are associated with flares near the western limb and SEP events seen by IMP 8 (Cane et al. 2002), range from 178° to halos. The three radio-silent CMEs have widths between 53° and 85°. No shock signature that can be traced back to these CMEs is seen near the Earth,

with the possible exception of 1998 Jan 03. The SOHO/MTOF monitor reports a shock signature on January 6th at 13:19 UT and one hour later, at 14:16UT, a moderate increase of the geomagnetic activity, identified as a Sudden Storm Commencement (SSC) is observed at the Earth. This shock could be triggered either by the CME under study or according to, e.g., Vilmer et al. (2003) by a halo CME ($v \sim 500$ km.s^{-1}) that is reported on January 2nd at 23:28. Is it possible that the CME-driven shock actually does accelerate SEP, but not on interplanetary field lines that are connected with SoHO, so that they are undetected by COSTEP? We note that EIT shows structural changes in the corona well into the visible solar disk (last column of Table 2), so that we expect that the CME extends into regions where the SoHO-connected field lines are rooted. The question then arises whether only the flanks of the shock, which presumably propagate slower and therefore are less efficient accelerators than the nose, intercept these well-connected field lines.

One can apply empirical corrections to estimate the intensity of SEP near the nose of the shock from the intensities or upper limits measured by COSTEP during the radio-silent CMEs. Kallenrode (1993) discusses multiple spacecraft observations of SEP events and derives characteristic scales for the decrease of the intensity of SEP events with longitudinal distance from the associated flare. If we attribute this decrease to the acceleration efficiency of a shock, the characteristic e-folding longitudinal distance of 13° for electrons, and a slightly smaller value for protons derived by Kallenrode (1993) implies that the intensity on an interplanetary field line connected at W 60° produced by a CME in the plane of the sky is about one order of magnitude below the intensity measured by an observer connected to the nose of the CME. But even if the measured low intensities were enhanced by an order of magnitude, the SEP events associated with the radio-silent CMEs would still be categorized as weak events.

In the light of the present results, the intense SEP events from the Kallenrode (1993) study presumably have large angular widths and flares associated with them. But there is no evidence in the present study that the shock waves driven by fast CMEs are able to accelerate conspicuous amounts of protons to energies of tens of MeV as observed in large SEP events. The large widths of the CMEs associated with major SEP events may be understood as a key to particle escape from the corona due to the large-scale restructuring of the magnetic field. Our study hence provides arguments that broaden the possible role of CMEs in SEP events beyond the usually invoked one as an accelerator.

3.4. Comments on radio-associated CMEs with weak or no SEP signatures

There are six fast CMEs of Table 1a, which do display radio signatures of coronal particle acceleration in the low and middle corona, but, like the radio-silent ones, have no clear SEP associated with them. One of them (event #7) occurs during an intense pre-existing event seen by ACE/EPAM. The electron and proton counts display a new rise near 14 UT on Apr 06 that might be ascribed to a new particle release in conjunction with the CME and the radio bursts. But the ongoing previous SEP event precludes the determination of the particle release time. Two other CMEs might be qualified as radio-silent, because they do not comprise a distinct burst, only a noise storm onset (# 23) or series of type III bursts which are likely associated with another noise storm (# 17). In order to avoid ambiguities, we prefer not to include these two cases into our list of radio-silent CMEs. Two of the three remaining CMEs (events # 5 and 14) are most probably associated with active regions behind the limb, which makes it plausible that particles accelerated in these regions do not reach the Earth. The last one, event #12 is ambiguous since according to Table 1a, it is associated with on disk activity located on the north western quadrant. However, a close examination of EIT and LASCO movies reveals that an active region in the south hemisphere and located behind the limb might be a possible candidate as well as the source of the CME. In summary, four and possibly five of the six CMEs which we did not classify as radio-silent are nonetheless consistent with the conclusion suggested from the radio-silent cases analysis that a fast CME is not a sufficient condition for a large SEP event to occur.

3.5. Summary and conclusion

In a systematic search for radio-silent fast CMEs, we clearly identified three events where metric radio emission behind the front of the CME is absent. The absence of radio signals precludes the presence of non-thermal electrons behind the CME, i.e. originating from processes in the lower corona. Thus, radio-silent fast CMEs provide the unique opportunity to test observationally the effectiveness of bare shock acceleration.

The observations of energetic particles associated with radio-silent CMEs have shown the absence of any conspicuous SEP event. Four scenarios are discussed that might explain this result: a) The CME is too slow for driving a sufficiently strong shock; b) the shock is fast enough, but encounters unfavorable conditions such as the lack of suprathermal seed particles; c) the radio-silent CME is too narrow, i.e. the field lines do not connect the observer with the shock as a precondition for observing energetic particles; and d) shock acceleration is too inefficient to provide conspicuous amounts of SEPs.

We conclude from our discussion that the absence of conspicuous SEP events after radio-silent CMEs on the western limb can hardly be ascribed to the speed of these CMEs or to the state of the corona. The speeds are to the best of our knowledge sufficient to drive a shock wave. Also, suprathermal seed populations are available in two of the three events.

However, the only apparent feature which distinguishes radio-silent CMEs from SEP-associated ones is the width. We cannot exclude that only the inefficient flank of the shock driven by radio-silent CMEs intercepts the Earth-connected interplanetary magnetic field line. But even after taking into account empirical results of the dependence of SEP intensity on the longitudinal distance between the presumed nose of the CME and spacecraft-connected longitudes, the SEP events of radio silent CMEs remain inconspicuous.

A systematic search during the rising phase of the activity cycle confirms that fast CMEs without signatures of particle acceleration in complex coronal magnetic field structures are rare. From our initial sample, all strong SEP events associated with fast CMEs are also accompanied by flares and by particle acceleration elsewhere than at the CME driven shock. Radio silent CMEs appear, in turn, as an intrinsically weak accelerator of escaping protons above 1 MeV. Quite evidently, this conclusion relies on a small number of radio silent events, but again the size of our final sample simply reveals how unusual pure events where one acceleration mechanism can be identified with certainty are. Indeed, it is not excluded that occasionally CME shocks accelerate protons up to a few tens of MeV, as concluded by Kahler et al. (1986) for the 1981 Dec 5 SEP event, but similarly, this single event remains exceptional and the present systematic study with a sensitive detector does not provide additional examples.

The conclusion suggested by this study does not mean that CMEs are irrelevant to SEP acceleration. The fact that, in large SEPs, both flare related particle acceleration in the low corona and large CMEs are observed, could indicate that the CME is the key to particle escape, rather than or in addition to particle acceleration. Systematic multi-spacecraft observations with STEREO and associated ground-based radio observations are a most promising tool to further our insight into the origin of SEP events.

This study made extensive use of data from the *WAVES/Wind* experiment, the GOES soft X-ray measurements, SoHO/EIT and SoHO/LASCO images and the LASCO CME catalogs compiled and maintained by O.C. ST. Cyr at Goddard Space Flight Center and by S. Yashiro at the Catholic University of America and GSFC. *YOHKOH/SXT* movies were also provided through the web site of the latter catalog. The SOHO/COSTEP project is supported under grant No. 50 OC 0105 by the German Bundesminister für Bildung und Forschung (BMBF) through the Deutsches Zentrum für Luft- und Raumfahrt (DLR).

SoHO is a project of international cooperation between ESA and NASA. The Nançay Radio Observatory is funded by the French Ministry of Education, the CNRS and the Région Centre. KLK thanks C. Gilbert for his considerable work on the event selection and the initial analysis. The authors would like to thank Y.-M Wang who kindly provided the software used in the magnetosonic speed estimates.

REFERENCES

Aschwanden, M. J. 2002, Spa. Sci. Rev., 101, 1

Bastian, T. S., Pick, M., Kerdraon, A., Maia, D., & Vourlidas, A. 2001, ApJ, 558, L65

Brueckner, G. E., Howard, R. A., Koomen, M. J., Korendyke, C. M., Michels, D. J., Moses, J. D., Socker, D. G., Dere, K. P., Lamy, P. L., Llbaria, A., Bout, M. V., Schwenn, R., Simnett, G. M., Bedford, D. K., & Eyles, C. J. 1995, Solar Phys., 162, 357

Cane, H. V., Erickson, W. C., & Prestage, N. P. 2002, JGR, 107, 1315

Cliver, E. W., Webb, D. F., & Howard, R. A. 1999, Sol. Phys., 187, 89

Delaboudinière, J. P., Artzner, G. E., Brunaud, J., Gabriel, A. H., Hochedez, J. F., Millier, F., Song, X. Y., Au, B., Dere, K. P., Howard, R. A., Kreplin, R., Michels, D. J., Moses, J. D., Defise, J. M., Jamar, C., Rochus, P., Chauvineau, J. P., Marioge, J. P., Catura, R. C., Lemen, J. R., Shing, L., Stern, R. A., Gurman, J. B., Neupert, W. M., Maucherat, A., Clette, F., Cugnon, P., & van Dessel, E. L. 1995, Solar Phys., 162, 291

Gold, R. E., Krimigis, S. M., Hawkins, S. E., Haggerty, D. K., Lohr, D. A., Fiore, E., Armstrong, T. P., Holland, G., & Lanzerotti, L. J. 1998, Space Science Reviews, 86, 541

Gopalswamy, N., Lara, A., Kaiser, M. L., & Bougeret, J.-L. 2001, JGR, 106, 25261

Gopalswamy, N., Yashiro, S., Krucker, S., Stenborg, G., & Howard, R. A. 2004, JGR, 109, A12105 (doi: 10.1029/2004JA01602)

Kahler, S., Reames, D., & Sheeley, N. 2001, ApJ, 562, 558

Kahler, S. W. 2001, J. Geophys. Res., 106, 20947

Kahler, S. W., Cliver, E., Cane, H., McGuire, R., Reames, D., Sheeley, N., & Howard, R. 1987, in Proc. 20th ICRC, Vol. 3, 121–123

Kahler, S. W., Cliver, E. W., Cane, H. V., McGuire, R. E., Stone, R. G., & Sheeley, N. R. 1986, 302, 504

Kahler, S. W., Sheeley, N. R., Howard, R. A., Michels, D. J., Koomen, M. J., McGuire, R. E., von Rosenvinge, T. T., & Reames, D. V. 1984, JGR, 89, 9683

Kallenrode, M. 1993, J. Geophys. Res., 98, 5573

Kerdraon, A. & Delouis, J. 1997, in LNP, Vol. 483, Coronal Physics from Radio and Space Observations, ed. G. Trottet (Springer), 192–201

Klassen, A., Bothmer, V., Mann, G., Reiner, M. J., Krucker, S., Vourlidas, A., & Kunow, H. 2002, A&A, 385, 1078

Klein, K.-L., Krucker, S., Trottet, G., & Hoang, S. 2005, A&A, in press

Klein, K.-L. & Posner, A. 2005, A&A, in press

Klein, K.-L., Schwartz, R. A., McTiernan, J. M., Trottet, G., Klassen, A., & Lecacheux, A. 2003, A&A, 409, 317

Labrador, A. W., Leske, R. A., Mewaldt, R., Stone, E., & von Rosenvinge, T. 2003, in Proc. 28th ICRC, Vol. 6, 3269–3272

Maia, D., Vourlidas, A., Pick, M., Howard, R., Schwenn, R., & Magalhães, A. 1999, JGR, 104, 12507

Mann, G., Classen, T., & Aurass, H. 1995, A&A, 295, 775

Mann, G., Klassen, A., Aurass, H., & Classen, H.-T. 2003, A&A, 400, 329

McLean, D. & Labrum, N. 1985, Solar radiophysics: studies of emission from the sun at metre wavelengths (Cambridge University Press)

Müller-Mellin, R., Kunow, H., Fleissner, V., Pehlke, E., Rode, E., Roschmann, N., Scharmberg, C., Sierks, H., Rusznyak, P., McKenna-Lawlor, S., Elendt, I., Sequeiros, J., Meziat, D., Sanchez, S., Medina, J., del Peral, L., Witte, M., Marsden, R., & Henrion, J. 1995, Solar Phys., 162, 483

Ogilvie, K. W., Chornay, D. J., Fritzenreiter, R. J., Hunsaker, F., Keller, J., Lobell, J., Miller, G., Scudder, J. D., Sittler, E. C., Torbert, R. B., Bodet, D., Needell, G., Lazarus, A. J., Steinberg, J. T., Tappan, J. H., Mavretic, A., & Gergin, E. 1995, Space Science Reviews, 71, 55

Pick, M. 1986, Solar Phys., 104, 19

Plunkett, S. P., Vourlidas, A., Šimberová, S., Karlický, M., Kotrč, P., Heinzel, P., Kupryakov, Y. A., Guo, W. P., & Wu, S. T. 2000, Solar Phys., 194, 371

Pohjolainen, S., Maia, D., Pick, M., Vilmer, N., Khan, J. . I., Otruba, W., Warmuth, A., Benz, A., Alissandrakis, C., & Thompson, B. . J. 2001, ApJ, 556, 421

Reames, D. V. 1999, Space Science Reviews, 90, 413

Reiner, M. J., Karlický, M., Jiřička, K., Aurass, H., Mann, G., & Kaiser, M. L. 2000, ApJ, 530, 1049

Richardson, I. G., Lawrence, G. R., Haggerty, D. K., Kucera, T. A., & Szabo, A. 2003, Geophys. Res. Lett., 30, 2 (doi: 10.1029/2002GL016424)

Sheeley, N. R., Howard, R. A., Michels, D. J., Robinson, R. D., Koomen, M. J., & Stewart, R. T. 1984, ApJ, 279, 839

Simnett, G. M., Roelof, E. C., & Haggerty, D. K. 2002, ApJ, 579, 854

Srivastava, N., Schwenn, R., & Stenborg, G. 1999, in 8th SoHO Workshop: Plasma Dynamics and Diagnostics in the Solar Transition Region and Corona, ESA SP No. 446, 621

St. Cyr, O. C., Howard, R. A., Sheeley, N. R., Plunkett, S. P., Michels, D. J., Paswaters, S. E., Koomen, M. J., Simnett, G. M., Thompson, B. J., Gurman, J. B., Schwenn, R., Webb, D. F., Hildner, E., & Lamy, P. L. 2000, JGR, 105, 18169

Tsuneta, S., Acton, L., Bruner, M., Lemen, J., Brown, W., Caravalho, R., Catura, R., Freeland, S., Jurcevich, B., & Owens, J. 1991, Sol. Phys., 136, 37

Vilmer, N. & MacKinnon, A. L. 2003, Lecture Notes in Physics, Berlin Springer Verlag, 612, 127

Vilmer, N., Pick, M., Schwenn, R., Ballatore, P., & Villain, J. P. 2003, Annales Geophysicae, 21, 847

Wang, Y.-M. 2000, ApJ, 543, L89

Wang, Y.-M. & Sheeley, N. R. 1992, ApJ, 392, 310

Warmuth, A., Hanslmeier, A., Messerotti, M., Cacciani, A., Moretti, P. F., & Otruba, W. 2000, Sol. Phys., 194, 103

Yashiro, S., Gopalswamy, N., Michalek, G., St. Cyr, O. C., Plunkett, S. P., Rich, N. B., & Howard, R. A. 2004, Journal of Geophysical Research (Space Physics), 7105